https://doi.org/10.5194/amt-2021-34
Preprint. Discussion started: 12 March 2021

Atmospheric Measurement Techniques Discussions

Rainfall retrieval algorithm for commercial microwave links: stochastic calibration

Wagner Wolff[1], Aart Overeem[2,3], Hidde Leijnse[2,3], and Remko Uijlenhoet[3,4]

[1]Department of Biosystems Engineering, University of São Paulo/"Luiz de Queiroz" College of Agriculture (ESALQ/USP);
[2]R&D Observations and Data Technology, Royal Netherlands Meteorological Institute (KNMI);
[3]Hydrology and Quantitative Water Management Group, Wageningen University & Research (WUR);
[4]Department of Water Management, Delft University of Technology (TU Delft).

Correspondence: Wagner Wolff (wwolff@usp.br)

Abstract. During the last decade, rainfall monitoring using signal level data from commercial microwave links (CMLs) in cellular communication networks has been proposed as a complementary way to estimate rainfall for large areas. Path-averaged rainfall is retrieved between the transmitting and receiving cellular antenna of a CML. One rainfall estimation algorithm for CMLs is RAINLINK, which has been employed in different regions (e.g., Brazil, Italy, the Netherlands, and Pakistan) with satisfactory results. However, the RAINLINK parameters have been calibrated for a unique optimum solution, which is inconsistent with the fact that multiple similar or equivalent solutions may exist due to uncertainties in algorithm structure, input data, and parameters. Here, we show how CML rainfall estimates can be improved by calibrating all parameters of the algorithm systematically and simultaneously with the stochastic optimization method Particle Swarm Optimisation, which is used for the numerical maximization of the objective function. An open dataset of approximately 2,800 sub-links of minimum and maximum received signal levels over 15-minute intervals covering the Netherlands (∼35,500 km^2) is employed, where 12 days are used for calibration and 3 months for validation. A gauge-adjusted radar rainfall dataset is utilized as reference. Verification of path-average daily rainfall shows a reasonable improvement for the stochastically calibrated parameters with respect to RAINLINK's default parameter settings. Results further improve when averaged over the Netherlands. Moreover, the method provides a better underpinning of the chosen parameter values and is therefore of general interest for calibration of RAINLINK's parameters for other climates and cellular communication networks.

1 Introduction

Accurate rainfall observations with high temporal and spatial resolution are crucial for, e.g., agriculture, meteorology, flood warnings and fresh water resource management. However, for many places on the earth's land surface, accurate rainfall information is lacking, especially from ground-based measurements at sub-daily and daily time scales (Sun et al., 2018). Another issue is the severe reduction in available ground-based measurements. For instance, the largest worldwide rain gauge database, maintained by the Global Precipitation Climatology Centre (GPCC), underwent a decline of approximately 43,000 (81%) and 27,000 (77%) rain gauges with monthly and daily precipitation records during the last 30 years, respectively (Schneider et al., 2018).

https://doi.org/10.5194/amt-2021-34
Preprint. Discussion started: 12 March 2021


Atmospheric Measurement Techniques Discussions

Suggested by Upton et al. (2005) and initially applied by Messer (2006) and Leijnse et al. (2007), the technique to estimate rainfall intensities based on signal level data from commercial microwave links (CMLs) is slowly but surely becoming a complementary source of rainfall information next to traditional ground-based measurements from rain gauges, weather radars and disdrometers. A CML is the link along a path between a transmitting antenna on one cell phone tower and a receiving antenna on another cell phone tower, often having two sub-links for communication in both directions. Since rainfall attenuates microwave radiation at frequencies of tens of GHz (wavelengths of about 1 cm), typically employed by CMLs, the integrated rain-induced attenuation along the link path can be computed from the decrease in signal levels with respect to dry weather, and subsequently converted to path-average rainfall. The core of the rainfall retrieval algorithm is the conversion of specific attenuation k (dB km^{-1}) to path-average rainfall intensity R (mm h^{-1}) via the power-law relation $R = ak^b$ (Atlas and Ulbrich, 1977; Olsen et al., 1978). The coefficient a (mm h^{-1} dB^{-b} km^b) and exponent b (–) depend mainly on the microwave link's frequency and polarization and on the rain drop size distribution (DSD) (Leijnse et al., 2007). Before applying the power-law relation, the received signal power must be processed to filter out any attenuation unrelated to rain, and to compare signals during a rainy interval with those from dry intervals. A typical workflow consists of: (i) CML data acquisition and preprocessing; (ii) identification of rain events in noisy raw data (wet-dry classification); (iii) baseline determination, representative of dry intervals; (iv) removal of outliers due to malfunctioning links; (v) correction of received signal powers; and (vi) computation of mean path-average rainfall intensities (Overeem et al., 2016a; Chwala and Kunstmann, 2019).

An advantage of CMLs is that they use the existing infrastructure of mobile network operators (MNOs) for network maintenance, data storage and acquisition. Furthermore, CMLs can be employed as a complement to existing rain gauge and weather radar networks, as well as in areas where instruments for ground observation are poor or non-existent. Thus, rainfall retrieval from CML data and subsequent mapping is a form of "opportunistic" sensing that has gained prominence in recent years (Uijlenhoet et al., 2018; Chwala and Kunstmann, 2019).

A number of studies highlight the successful employment of CMLs for rainfall retrieval, of which the most relevant for this study are discussed here. Zinevich et al. (2009) show that this technique is suitable for measuring near-ground rainfall around the cities of Ramle and Modi'in (area $\approx$ 900 km^2; density $\approx$ 0.025 CML km^{-2}) in Israel. Studying the alpine and pre-alpine regions of Southern Germany (area $\approx$ 1200 km^2; density $\approx$ 0.0042 CML km^{-2}), Chwala et al. (2012) reached high correlations for both CML–rain gauge and CML–rain radar comparison. Incorporating the uncertainty associated with the different sources of rainfall information, Bianchi et al. (2013) obtained reliable rainfall intensity estimates by combining rain gauge, radar, and microwave link observations in the Zürich area, Switzerland (area $\approx$ 460 km^2; density $\approx$ 0.03 CML km^{-2}). In a dedicated case study in Prague, Czech Republic, Fencl et al. (2015) used 14 CMLs over a small area of 2.5 km^2 (i.e. a density of 5.6 CML km^{-2}), concluding that quantitative precipitation estimates from CMLs capture the spatio-temporal rainfall distribution at the microscale very well. Recently, de Vos et al. (2019) reached correlations around 0.60 for daily rainfall accumulations, using instantaneously sampled data from a CML network in the Netherlands (density $\approx$ 0.054 CML km^{-2}). Moreover, comparing those results with earlier studies in the Netherlands, the authors highlight min/max sampling outperforms instantaneous sampling in terms of rainfall estimates. Long-term studies involving country-wide verification of CML rainfall estimates based on data from a few thousand CMLs are provided by Overeem et al. (2016b) for the Netherlands employing RAINLINK 1.2 (Overeem

https://doi.org/10.5194/amt-2021-34
Preprint. Discussion started: 12 March 2021


Atmospheric Measurement Techniques Discussions

et al., 2016a), and by Graf et al. (2020) for Germany employing pycomlink (https://github.com/pycomlink/pycomlink), both open-source rainfall retrieval algorithms.

Likewise, research has been conducted to evaluate CML-derived rainfall in hydrological model responses. Brauer et al. (2016) study the effects of differences in rainfall measurement techniques (including CMLs) on discharge and groundwater simulations using a lumped rainfall-runoff model in a small (6.5 km^2) catchment. CML-derived rainfall estimates are found to lead to much better results than real-time weather radar data when comparing discharge and groundwater simulations to observations for a full year. Investigating the potential of CML-derived rainfall estimates for streamflow prediction and water balance analyses, Smiatek et al. (2017) observe a significant improvement in the reproduction of observed discharge values for events with local heavy rainfall. The authors find that even rainfall fields provided by gauge-adjusted weather radar do not capture such events, which suggests that an extremely dense monitoring network would be needed to properly capture local heavy rainfall. Likely, this explains why Liberman et al. (2014) achieve better results by merging CML and radar data rather than using just one of these sources to retrieve rainfall intensities.

Despite all these studies showing the potential of CMLs for rainfall monitoring, challenges remain. These are mainly related to dealing with typical sources of error, e.g., wetting of antennas in rain events causing additional attenuation and hence resulting in rainfall overestimation, as well as signal level decrease during dry periods in CML raw data (Leijnse et al., 2008; Messer and Sendik, 2015; Overeem et al., 2016a). Rainfall retrieval algorithms for CMLs aim to take these phenomena into account, although issues such as wet-dry classification still require improvement. Another challenge concerns the calibration of the parameters of the rainfall retrieval algorithms. Current calibration procedures fall short of addressing the uncertainties associated with CML signal levels (e.g. due to different brands of antennas and varying path lengths), algorithm structure (e.g. attenuation thresholds for classification of rainy and nonrainy periods), model parameters (e.g. for wet antennas and outlier filters), and rainfall itself (e.g. due to DSD spatial variability along the link path). Concretely, the parameters of the algorithms are calibrated empirically in order to obtain a unique optimum solution. The most precise path-averaged rainfall intensity estimates will be obtained using these optimized parameter sets (Matott et al., 2009).

Here, we partly address this by calibrating the most important parameters of the open-source rainfall retrieval algorithm RAINLINK systematically and simultaneously with the stochastic optimization method Particle Swarm Optimisation. This is preceded by a sensitivity analysis selecting the most important parameters. RAINLINK has been used for CML rainfall estimation in various regions, i.e. Brazil, Italy, the Netherlands, Nigeria, Pakistan, and Sri Lanka (Overeem et al., 2016a, b; Sohail Afzal et al., 2018; Rios Gaona et al., 2018; de Vos et al., 2019; GSMA, 2019; Roversi et al., 2020), and has been calibrated deterministically (Overeem et al., 2011, 2013, 2016a, b; de Vos et al., 2019). With the new optimization method we provide a better underpinning of parameter values for this CML rainfall retrieval algorithm. These resulting CML rainfall estimates are contrasted to those based on RAINLINK's default parameter values (Overeem et al., 2011, 2013, 2016a). A gauge-adjusted radar rainfall dataset is utilized as reference for the CML-derived path-average rainfall estimates. We use a large publicly available CML dataset of approximately 2,800 sub-links of minimum and maximum received signal levels over 15-minute intervals covering the Netherlands ($\sim$ 35,500 km^2), where 12 days are used for calibration and 3 months for validation.

https://doi.org/10.5194/amt-2021-34
Preprint. Discussion started: 12 March 2021


Atmospheric Measurement Techniques Discussions

This study is organized as follows. First, study area (Section 2.1), datasets (Section 2.1), and methodology (Sections 2.2 and 2.3) employed for RAINLINK calibration are presented. Next, the results and discussion (Section 3) present our major findings. Finally, the conclusions (Section 4) summarize the findings and highlight the recommendations and outlooks for further research.

2 Material and methods

2.1 Study area and datasets

The study area considered is the Netherlands ($\sim$ 35,500 km^2; Fig. 1 (a)), which has a temperate oceanic climate according to the Köppen-Geiger classification (Peel et al., 2007). CML data were obtained from MNO T-Mobile NL: minimum and maximum received powers over 15-minute intervals, based on 10 Hz sampling with a precision of 1 dB. Data from approximately 2,800 sub-links (validation) and 2,940 (calibration) per time interval were available (after preprocessing with RAINLINK). The 12-day calibration dataset, used to optimize RAINLINK's parameters, covers the period from June to September 2011. It served as validation dataset in Overeem et al. (2013). The 3-month validation dataset covers the summer months June, July, and August 2012. We are only using data from summer in the Netherlands to prevent analyzing events with solid precipitation. This has the added advantage of the data bearing greater resemblance to rainfall in (sub)tropical climates, where the use of CMLs for rainfall retrieval has the largest potential.

Figure 1 illustrates the main characteristics of the CML dataset used for validation. Being distributed over the entire country (Fig. 1 (a)), the CMLs have a high temporal and spatial data availability, i.e., 92% of CMLs have observations for more than 80% of the period. In spite of not having a perfectly uniform distribution in terms of their directions, all direction classes are well-represented (Fig. 1 (b)). Microwave frequencies range from $\sim$13 GHz to 40 GHz (the majority from 37 to 40 GHz, Fig. 1 (c)). Lengths vary from 0.1 km to 20 km (the majority less than 5 km, Fig. 1 (d)), where shorter lengths typically correspond to higher microwave frequencies (Fig. 1 (d)).

A climatological gauge-adjusted radar rainfall dataset of 5-min rainfall depths, aggregated over 15 minutes, was used as reference for calibration of the rainfall retrieval algorithm (RAINLINK) and validation of rainfall estimates. The radar dataset is maintained by the Royal Netherlands Meteorological Institute (KNMI) and has a 1-km spatial resolution. For more details see Overeem et al. (2009a, b, 2011).

2.2 Rainfall retrieval algorithm

Overeem et al. (2016a) describes the CML rainfall retrieval algorithm RAINLINK. Made available as R-package (R Core Team, 2018), RAINLINK (Overeem et al., 2019) is hosted via GitHub at website https://github.com/overeem11/RAINLINK. RAINLINK's default parameter values are derived or selected in (Overeem et al., 2011, 2013, 2016a). The algorithm begins with a quality control by preprocessing of the CML data. Links with frequencies lower than 12.5 GHz and higher than 40.5 GHz are discarded. Moreover, the attributes frequency, link coordinates, path length, and identifier are checked for either duplicated

https://doi.org/10.5194/amt-2021-34
Preprint. Discussion started: 12 March 2021

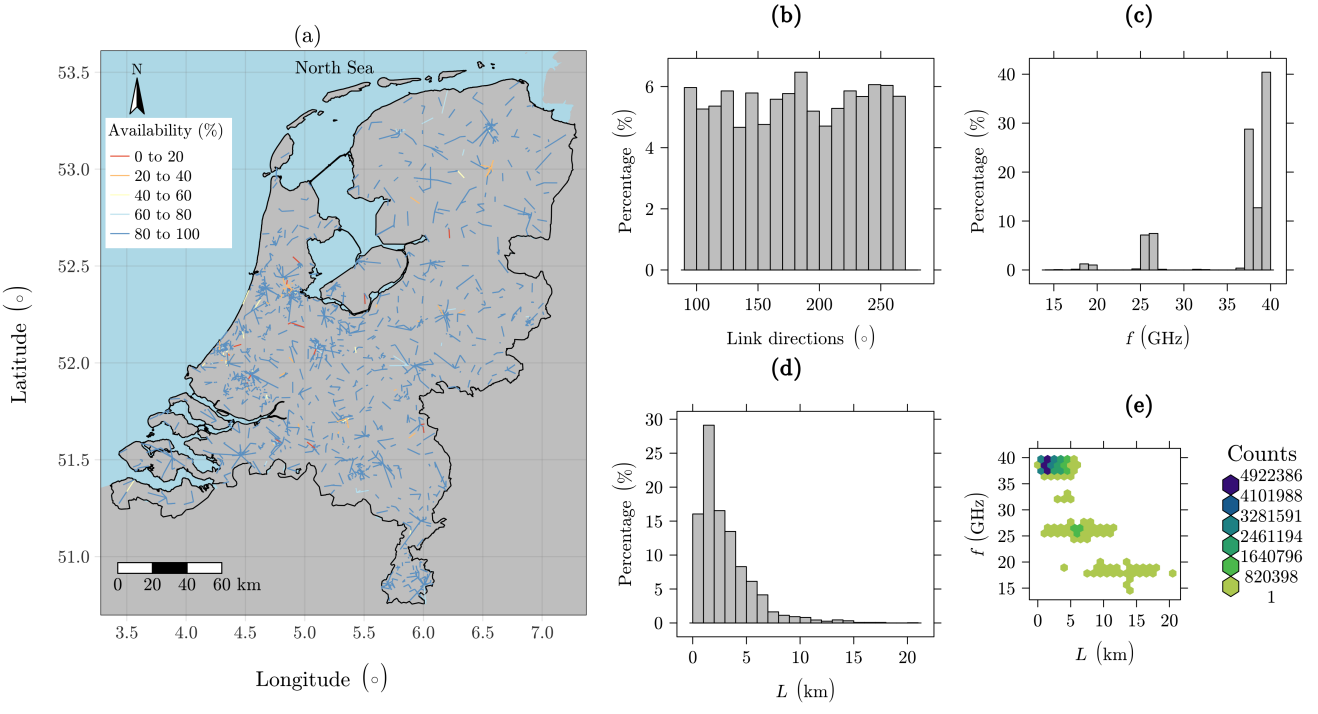

Figure 1. Map of the Netherlands and sub-link characteristics for the validation dataset: (a) CML locations and availability, (b) distribution of link directions, (c) distribution of microwave link frequencies, (d) distribution of link lengths, and (e) density of link length and frequency combinations.

or mismatches of information. Next, RAINLINK is divided into two main sub-processes, one for defining wet and dry periods and the other one for the actual rainfall retrieval.

2.2.1 Wet-dry classification

The process to define wet and dry periods assumes that rainfall is spatially correlated. Therefore, during a rainy time interval, a substantial decrease in received signal levels should be detected by nearby links within a specific radius (Overeem et al., 2011, 2016a). This approach is called “nearby link approach”. The output is a binary response to indicate wet and dry periods, respectively. Table 1 highlights all employed parameters.

2.2.2 Rainfall retrieval

Once the rainy and non-rainy time intervals have been identified, a reference signal level (P_{ref}) is computed, which represents the median received power during dry intervals. Next, outliers are removed by applying a filter which uses specific attenuation derived from the uncorrected minimum received power. It assumes that rainfall is correlated in space. The filter removes a time

https://doi.org/10.5194/amt-2021-34
Preprint. Discussion started: 12 March 2021

Atmospheric Measurement Techniques Discussions

Table 1. Wet-dry classification parameters (WD_{pn}): default values from RAINLINK and calibration search space (minimum and maximum values). Modified from Overeem et al. (2016a).

Parameter description	Symbol and unit	Default value	Minimum value	Maximum value
WD_{p1} – Minimum number of hours needed to compute max(P_{min})	– (h)	6	2	10
WD_{p2} – Number of previous hours over which max(P_{min}) is to be computed (also determines period over which cumulative difference F of outlier filter is computed)	– (h)	24	6	24
WD_{p3} – Radius	r (km)	15	15	30
WD_{p4} – Attenuation threshold	median(ΔP) (dB)	-1.4	-5	0
WD_{p5} – Specific attenuation threshold	median(ΔP_L) (dB km^{-1})	-0.7	-2	0
WD_{p6} – Minimum number of available (surrounding) links	– (–)	3	3	10
WD_{p7} – Minimum received power threshold	– (dB)	2	1	4

interval of a link for which the time-integrated difference between its specific attenuation and that of the surrounding links over the previous period (Tab. 2, parameter RR_{p2}) is lower (i.e. more negative) than a certain threshold (Tab. 2, parameter RR_{p3}).

Preventing nonzero rainfall estimates during non-rainy intervals, corrected minimum (P^{C}_{min}) and maximum (P^{C}_{max}) received powers are calculated by adjusting the signals to the base level for non-rainy intervals. Subsequently, the minimum and maximum rain-induced attenuation, A_{min} (dB) and A_{max} (dB), respectively, are calculated for each link and time interval using

$$\begin{aligned} A_{min} &= P_{ref} - P^{C}_{max}, \\ A_{max} &= P_{ref} - P^{C}_{min}. \end{aligned} \tag{1}$$

Next, the minimum and maximum path-averaged rainfall intensities, $\overline{R}_{min}$ (mm h^{-1}) and $\overline{R}_{max}$ (mm h^{-1}), respectively, are computed according to

$$\overline{R}_{min,\,max} = a \left(\frac{A_{min,\,max} - A_a}{L} H\left(A_{min,\,max} - A_a\right) \right)^b, \tag{2}$$

where H is the Heaviside function (if the argument of H is smaller than zero, $H = 0$; else $H = 1$). A_a (dB) is a fixed wet antenna attenuation correction term, and a (mm h^{-1} dB^{-b} km^{b}) and b (-) are the coefficient and exponent of the employed power-law $R - k$ relation, respectively. The values of a and b, which depend mainly on link frequency, have been derived from measured raindrop size distributions and computations of electromagnetic scattering by rain drops for vertically polarized signals (Leijnse et al., 2008). The polarization for individual links was unknown, but the majority of links used vertically polarized signals.

Finally, the mean path-averaged rainfall intensity, $\overline{R}$ (mm h^{-1}) is computed by means of

$$\overline{R} = \alpha \overline{R}_{max} + (1 - \alpha)\, \overline{R}_{min}, \tag{3}$$

https://doi.org/10.5194/amt-2021-34
Preprint. Discussion started: 12 March 2021

Atmospheric Measurement Techniques Discussions

Table 2. Rainfall retrieval parameters (RR_{pn}): default values from RAINLINK and calibration search space (minimum and maximum values). Modified from Overeem et al. (2016a).

Parameter description	Symbol and unit	Default value	Minimum value	Maximum value
RR_{p1} – Minimum number of hours that should be dry in preceding period	– (h)	2.5	2.5	12
RR_{p2} – Period over which reference level is to be determined	– (h)	24	12	24
RR_{p3} – Outlier filter threshold	F_t (dB km^{-1} h)	-32.5	-100	0
RR_{p4} – Wet antenna attenuation	A_a (dB)	2.3	0	5
RR_{p5} – Temporal rainrate distribution coefficient	α (–)	0.33	0.1	0.6

where α is a coefficient which determines the contribution of the minimum and maximum path-averaged rainfall intensity during a time interval. Table 2 gives an overview of all parameters used in the rainfall retrieval process.

2.3 RAINLINK sensitivity analysis and calibration

Using the 15-minute rainfall accumulations retrieved from RAINLINK, the parameters with the highest importance in the algorithm are identified by means of a sensitivity analysis called Latin-Hypercube One-factor-At-a-Time (LH-OAT) (Van Griensven et al., 2006). This method ensures that the full range of parameters is sampled according to a LH design and within each sample the parameters are tested, one at a time. Initially, it takes N LH sample points for N intervals while varying each LH sample point p times by changing each of the p parameters one at a time, according to the OAT design (Van Griensven et al., 2006). Around each Latin Hypercube point a relative partial effect for each parameter is calculated. A final effect is calculated by averaging the partial effects over all N LH points.

The method is very efficient, as the N intervals in the LH method require a total of $N(p+1)$ evaluations. The relative importance of the parameters is determined by ranking the final effects from large to small (Van Griensven et al., 2006). Each relative importance can be divided by the sum of all relative importances to yield a normalized measure of relative importance. The twelve parameters selected for the sensitivity analysis are listed in Tables 1 and 2. The most sensitive parameters are selected such that the sum of their normalized relative importances reaches at least 85%.

After having selected the most important parameters by sensitivity analysis, the RAINLINK parameters are optimized with the method Standard Particle Swarm Optimization (SPSO-2011) (Clerc, 2012). SPSO-2011 is a stochastic, effective, and efficient calibration method, as highlighted in recent studies with other hydrological and environmental models (Abdelaziz and Zambrano-Bigiarini, 2014; Bisselink et al., 2016; Pijl et al., 2018). The optimization is performed for the two RAINLINK subprocesses separately. First, the wet-dry classification parameters are calibrated, to make sure RAINLINK is able to correctly identify dry and rainy periods. Next, using the optimum parameters for the wet-dry classification, the rainfall retrieval parameters are calibrated. We have included all zero rainfall observations in the entire calibration process, both for the gauge-adjusted

https://doi.org/10.5194/amt-2021-34
Preprint. Discussion started: 12 March 2021


Atmospheric Measurement Techniques Discussions

radar reference and for the RAINLINK estimates. Note that data from individual sub-links were used in the calibration process, so data from two links (in opposite directions) having the same link path were not averaged.

The goodness-of-fit measures chosen to drive the optimization and performance for the wet-dry classification and the rainfall retrieval are the simple matching (SM) (Sokal and Michener, 1958) and the modified Kling-Gupta efficiency (KGE) (Kling et al., 2012), respectively. Both are maximized towards an optimum value of 1. A 15-minute time interval from a given sub-link is classified as dry if the reference is 0 mm. SM is defined as

$$\mathrm{SM} = \frac{d+w}{n}, \tag{4}$$

where d is the number of links classified correctly as dry, w is the number of links classified correctly as wet, and n is the total number of links. KGE is defined as

$$\mathrm{KGE} = 1 - \sqrt{(\rho-1)^2 + (\beta-1)^2 + (\gamma-1)^2}, \tag{5}$$

with ρ the Pearson correlation coefficient, β the bias ratio

$$\beta = \frac{\mu_\mathrm{e}}{\mu_\mathrm{o}}, \tag{6}$$

and γ the variability ratio

$$\gamma = \frac{\mathrm{CV_e}}{\mathrm{CV_o}} = \frac{\sigma_\mathrm{e}\mu_\mathrm{o}}{\mu_\mathrm{e}\sigma_\mathrm{o}}, \tag{7}$$

where μ and σ are the mean and standard deviation of path-averaged rainfall intensity (mm h^{-1}) for CML estimates (e) and gauge-adjusted radar observations (o). CV is the coefficient of variation, defined as the ratio of the standard deviation and the mean.

In addition to KGE and its components ρ, β and γ, the CV of the residuals ($\mathrm{CV_{res}}$), the percent bias (PBIAS) and root-mean-square error (RMSE) are employed in the validation phase to evaluate the performance of RAINLINK in terms of its rainfall estimates using the newly calibrated parameters against its default parameters:

$$\mathrm{CV_{res}} = \frac{\sigma_\mathrm{res}}{\mu_\mathrm{o}}, \tag{8}$$

$$\mathrm{PBIAS} = 100\frac{\sum_{i=1}^{n}(\mathrm{e}_i - \mathrm{o}_i)}{\sum_{i=1}^{n}\mathrm{o}_i}, \tag{9}$$

$$\mathrm{RMSE} = \sqrt{\frac{\sum_{i=1}^{n}(\mathrm{e}_i - \mathrm{o}_i)^2}{n}}. \tag{10}$$

https://doi.org/10.5194/amt-2021-34
Preprint. Discussion started: 12 March 2021

Atmospheric Measurement Techniques Discussions

Table 3. Wet-dry classification sensitivity analysis: WD_{pn} (symbol) – wet-dry classification parameters, see description in Table 1. Note: [a] - Most sensitive parameters obtained from the Latin-Hypercube One-factor-At-a-Time analysis.

Rank	Parameter (symbol)	Relative Importance (RI)	RI Normalized
1[a]	WD_{p5} (median(ΔP_L))	3.16	0.44
2[a]	WD_{p4} (median(ΔP))	2.37	0.31
3[a]	WD_{p1}	1.04	0.13
4	WD_{p3} (r)	0.48	0.065
5	WD_{p2}	0.36	0.044
6	WD_{p7}	0.35	0.040
7	WD_{p6}	0.014	0.002

Finally, the level of agreement of daily rainfall patterns is analyzed graphically. Jointly with a scatter density plot a linear regression is performed between the estimated and observed path-averaged rainfall depths (mm) and its deviation from the 1:1 line is evaluated. RAINLINK's ability to estimate 15-minute path-average rainfall rates is also evaluated. Moreover, both agreement of accumulated rainfall for all individual CMLs and agreement of daily mean rainfall over the Netherlands (as time series) are considered, taking those links with over 80% of data availability into account.

3 Results and discussion

3.1 Calibration

3.1.1 Wet-dry classification parameter optimization

The sensitivity analysis for the wet-dry classification process is performed at a 15-minute time interval. Table 3 provides the parameter ranking obtained considering the search space illustrated in Tab. 1. The most important parameters are those related to the threshold of attenuation, WD_{p4} (median(ΔP)) and specific attenuation, WD_{p5} (median(ΔP_L)), as well as the minimum number of hours needed to compute the maximum of the minimum received power, WD_{p1}. The accumulated relative importance of these parameters is 88%. The importance of the two thresholds was expected, because these parameters define the values for which an individual microwave link will be classified as rainy or not. However, the analysis performed here, which systematically evaluates all parameters together by maximizing a goodness-of-fit measure, reveals that the parameter WD_{p1} is important as well. The low ranking of the WD_{p7} threshold is consistent with the findings of Overeem et al. (2016a), who report that including this step hardly changes results for a 12-day dataset when validating rainfall depths (i.e., the total effect on the amounts, not the occurrence of wet and dry periods as such).

The three highest ranked parameters are now employed in the calibration, taking the ranges reported in Tab. 1 into account. Using particle swarm optimization (PSO), the parameters' dispersion and distributions across the search space have been computed for the 12-day calibration dataset (Fig. 2). The distributions are obtained for the "behavioral" solutions, i.e., for those parameter sets for which the simple matching (SM) metric (Eq. 4) is higher than 0.90. This threshold value is obtained by

https://doi.org/10.5194/amt-2021-34
Preprint. Discussion started: 12 March 2021


Atmospheric Measurement Techniques Discussions

using the default parameters in the wet-dry classification process. The frequency histograms of the parameters are multi-modal and skewed (Fig. 2b), reflecting the uncertainties in the optimum values.

The Wilcoxon signed rank test is employed for obtaining the median and 95% confidence intervals around the optimum parameter values (Wilcoxon, 1945). The parameters WD_{p1}, $\mathrm{WD}_{\mathrm{p4}}$, and $\mathrm{WD}_{\mathrm{p5}}$ reach optimum values equal to 4.52 h, -1.81 dB, and -0.80 dB km^{-1}, respectively. Compared with the default values of these parameters, namely 6 h, -1.4 dB and -0.7 dB km^{-1}, the difference is small for the parameters $\mathrm{WD}_{\mathrm{p4}}$ and $\mathrm{WD}_{\mathrm{p5}}$. However, the parameter $\mathrm{WD}_{\mathrm{p1}}$ is found to be 1.5 hour less than the default value. Thus, the maximum of the minimum received power ($\max(P_{\mathrm{min}})$) for the nearby microwave links is computed for a shorter time interval. Considering the "behavioral" solutions, the 95% confidence intervals are [4.44, 4.62], $[-1.84, -1.78]$, and $[-0.81, -0.79]$ for the parameters $\mathrm{WD}_{\mathrm{p1}}$, $\mathrm{WD}_{\mathrm{p4}}$, and $\mathrm{WD}_{\mathrm{p5}}$, respectively.

For the wet-dry classification employing the calibrated parameters, the simple matching measure reaches a mean value equal to 0.9, i.e., 90% of the microwave links provide a correct wet-dry classification considering the entire period of 12 days. It should be noted that, in spite of being gauge-adjusted, the radar product used here is not a perfect reference. Differences between radar sampling (indirect measurements aloft) and ground-based sensors can lead to significant errors (de Vos et al., 2019). Thus, accounting for this sampling difference could even further increase the value of the simple matching metric. In particular for small rainfall events these errors can lead to false positive and false negative classifications.

Although by applying the default parameters the same value of SM is obtained, due to the higher value of $\mathrm{WD}_{\mathrm{p1}}$ 12% of the microwave link data are excluded during the algorithm processing, while only 7% are excluded when employing the calibrated parameters. In other words, the proposed calibration procedure leads to the same performance, but yields rainfall estimates for more CML locations.

3.1.2 Rainfall retrieval parameter optimization

The same sensitivity analysis and calibration are employed for the rainfall retrieval at the 15-minute time interval (Tab. 4), where zeroes in either CML and/or reference are also included. The sensitivity analysis presented here underlines the uncertainty associated with the microwave link measurements. The most sensitive parameters are the parameters RR_{p4} (A_{a}), $\mathrm{RR}_{\mathrm{p5}}$ (α), and $\mathrm{RR}_{\mathrm{p3}}$ (F_{t}). The summed relative importance of these parameters is 85%.

The parameter $\mathrm{RR}_{\mathrm{p4}}$ is related to the correction of the attenuation due to wet antennas. This phenomenon is considered an important source of extra attenuation and may cause significant rainfall overestimation if not sufficiently accounted for (Leijnse et al., 2008; Messer and Sendik, 2015; Overeem et al., 2016a).

Since the parameter $\mathrm{RR}_{\mathrm{p5}}$ represents a coefficient that determines the relative contributions of the minimum and maximum path-averaged rainfall intensities ($\overline{R}_{\mathrm{min}}$ and $\overline{R}_{\mathrm{max}}$, Eq. 3) to the 15-minute average rainfall intensity estimates, it is directly related to the temporal sampling strategy of the received signal power and has an important weight in the rainfall retrieval. In a comparative study, de Vos et al. (2019) found that min/max sampling at a 15-minute time step (as employed by RAINLINK) outperforms instantaneous sampling in the Dutch climate. This underlines the importance of properly estimating $\mathrm{RR}_{\mathrm{p5}}$ (α) for accurate rainfall retrievals.

https://doi.org/10.5194/amt-2021-34
Preprint. Discussion started: 12 March 2021

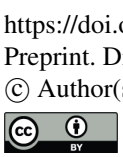

Atmospheric Measurement Techniques Discussions

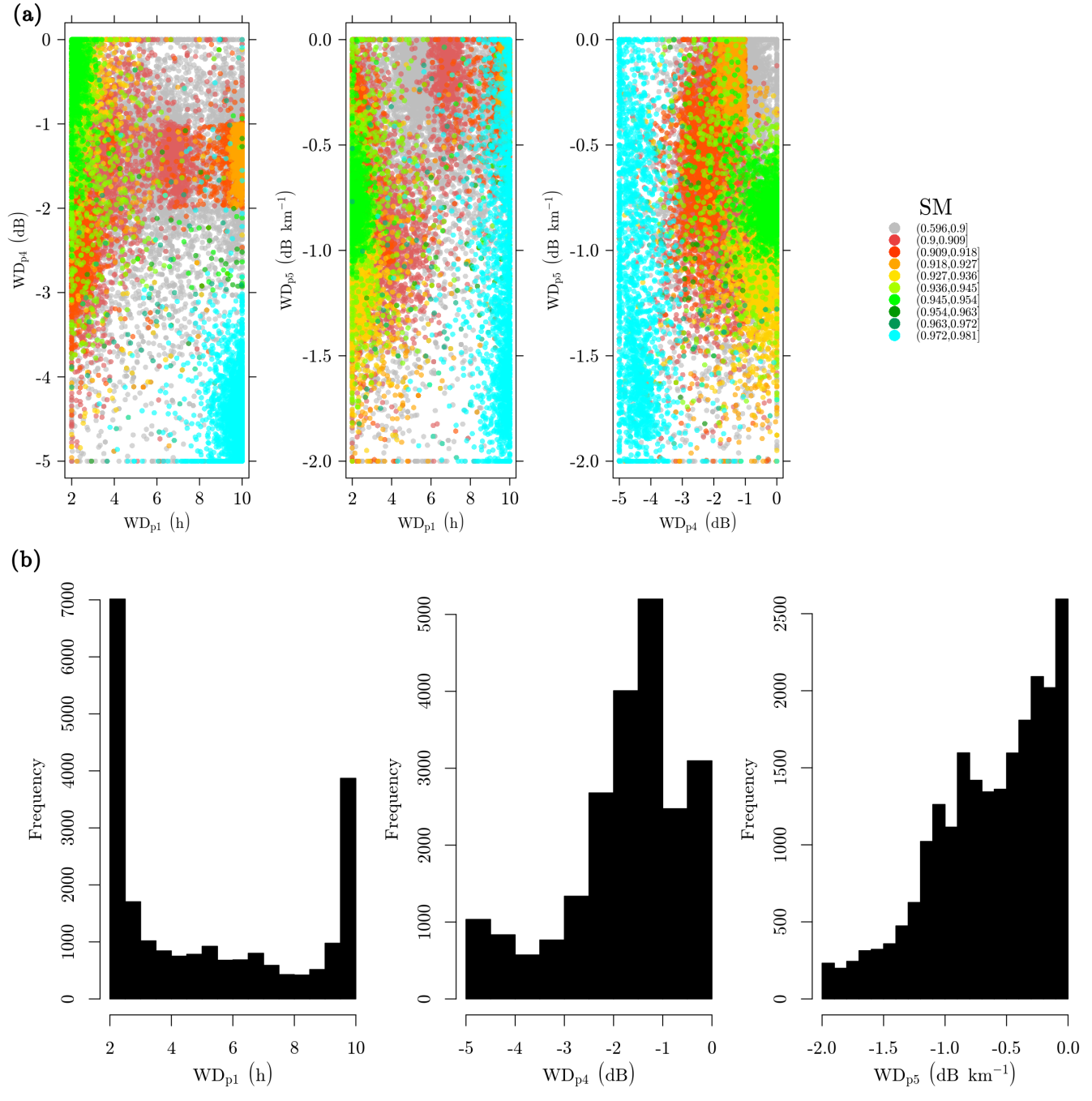

Figure 2. Calibration of the wet-dry classification parameters: (a) dotty plot showing the interaction between calibration parameters at different simple matching (SM) values; (b) histograms of the parameters for the "behavioral" solutions.

https://doi.org/10.5194/amt-2021-34
Preprint. Discussion started: 12 March 2021

Atmospheric Measurement Techniques Discussions

Table 4. Rainfall retrieval sensitivity analysis: RR_{pn} – rainfall retrieval parameters, see Tab. 2.

Rank	Parameter (symbol)	Relative Importance (RI)	RI Normalized
1	RR_{p4} (A_a)	774	0.55
2	RR_{p5} (α)	350	0.20
3	RR_{p3} (F_t)	187	0.10
4	RR_{p1}	130	0.06
5	RR_{p2}	46.6	0.03

The parameter RR_{p3} (F_t) represents an outlier filter. Therefore, it seems reasonable to assume a threshold value based on expert judgment, because strict filtering would result in a high performance, but with a severe decline in the remaining number of links. Using the default values of the parameters RR_{p4} (A_a) and RR_{p5} (α) obtained in Overeem et al. (2013), Overeem et al. (2016a) applied a sensitivity analysis varying only the parameter RR_{p3} (F_t), confirming that the default value equal to -32.5 dB km^{-1} h^{-1} (Overeem et al., 2013) is a reasonable trade-off between performance and retaining a significant number of links. Therefore, even though a proper calibration procedure is deemed important, the default value of RR_{p3} (F_t) fixed at -32.5 dB km^{-1} h^{-1} is kept to prevent an excessive loss of data.

Figure 3 illustrates the interaction between parameters in the calibration procedure for the rainfall retrieval at different KGE-values. This figure shows that the regions with the highest KGE-values (greens and blue points) correspond mainly to values ranging from 1 to 3 dB for RR_{p4} and from 0.1 to 0.3 for RR_{p5}. Using the default RAINLINK parameters, a KGE value equal to 0.67 is obtained. This value is used as a threshold for the "behavioral" solutions (gray points in Fig. 3). A strong variability among the possible best solutions is observed, as the "behavioral" samples are widely spread within the parameter search space, with maximum values equal to 1.71 dB and 0.21 for RR_{p4} and RR_{p5}, respectively. According to the Wilcoxon signed rank test (Wilcoxon, 1945), the 95% confidence intervals for the parameters RR_{p4} and RR_{p5} are [1.62, 1.80] and [0.20, 0.22], respectively, which is in line with what can be seen in Fig. 3.

The parameter RR_{p4} shows a a more pronounced dispersion than the parameter RR_{p5}. RR_{p4} is related to wet antenna attenuation and varies depending on the ambient conditions, e.g. while there is dew, rain water or melting precipitation (the latter unlikely in this study) present on the antenna covers (Leijnse et al., 2008; Overeem et al., 2016b; Uijlenhoet et al., 2018). It may also vary depending on the type of antenna cover. Finally, in the rainfall retrieval algorithm it is always assumed that, whenever it rains, both antennas of a microwave link are wet, whereas in reality none or only one antenna may be wet. Hence, it is unlikely that all CMLs across the considered study area will share the same excess signal attenuation in terms of magnitude, timing and spatial occurrence. In principle, each single CML is expected to have its own time-varying set of values of the parameter RR_{p4}. This implies great uncertainty in the overall optimum value for the time period and region of interest.

It is apparent from Fig. 3 that the parameter RR_{p5} reaches its optimum value at 0.21, which is much lower than RAINLINK's default value of 0.33. This implies that the maximum and minimum path-averaged rainfall intensities ($\overline{R}_{max}$, $\overline{R}_{min}$) have respective weights of 0.21 and 0.79 in the computation of the best estimate of the 15-minute mean path-averaged rainfall intensity. However, a smaller spread around the optimum value compared to the other parameters can be observed, indicating a moderate uncertainty around the optimum. Note that the value of α is related to the temporal distribution of path-average rainfall intensi-

https://doi.org/10.5194/amt-2021-34
Preprint. Discussion started: 12 March 2021

Atmospheric Measurement Techniques Discussions

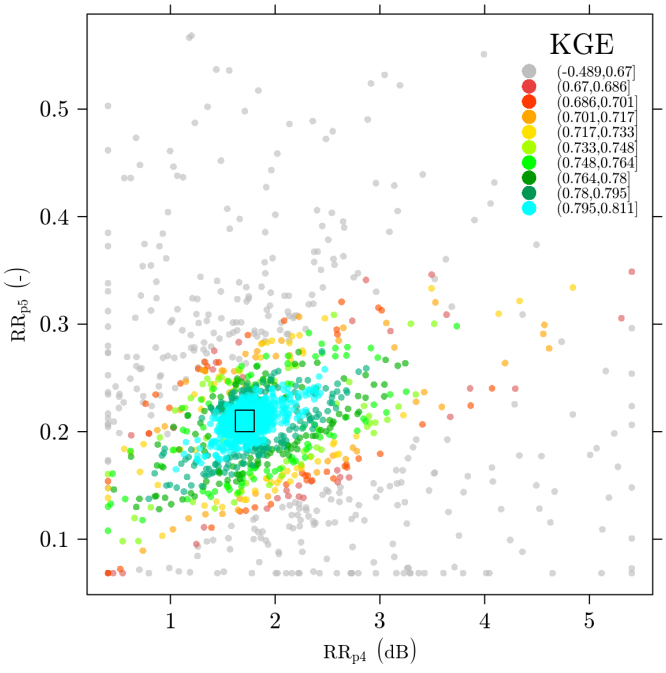

Figure 3. Rainfall retrieval performance projected onto the parameter space: dotty plot showing the interaction between calibration parameters at different KGE-values. The grey dots represent solutions corresponding to KGE-values below 0.67, i.e. the "behavioral" solutions are above this threshold, whereas the black rectangle represents the 95% confidence intervals.

ties within 15-minute intervals, which is influenced by the lengths of the links as well as by the rainfall space-time variability. This suggests that the optimum parameter value will depend on both link network topology and rainfall climatology.

3.2 Validation

After the parameter optimization using the 12-day calibration dataset from 2011, the optimized and default parameter sets are applied to a 3-month validation dataset from July, August, and September 2012. The 15-minute path-average rainfall estimates were aggregated to hourly and daily path-average rainfall estimates if CML-availability was at least 80%, resulting in data from on average 2,334 and 2,339 sub-links for the default and optimized parameters, respectively. Thus, given that after the RAINLINK pre-processing on average 2,951 sub-links are left, data availability reduces by approximately 21% for both default and optimized parameters.

Figure 4 illustrates the performance in terms of daily path-average rainfall estimates for the two tested parameter sets, i.e., calibrated and default. In general, the metrics for the calibrated parameters are slightly better than those for the default parameters. The values improve from 0.45 to 0.49 for KGE, from 6.2 mm to 5.63 mm for RMSE, and from 2.29 to 2.09 for CV_{res}, whereas (ρ) is slightly better (0.52 vs. 0.51) for the default parameters.

https://doi.org/10.5194/amt-2021-34
Preprint. Discussion started: 12 March 2021

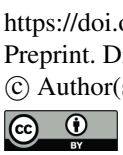

Atmospheric Measurement Techniques Discussions

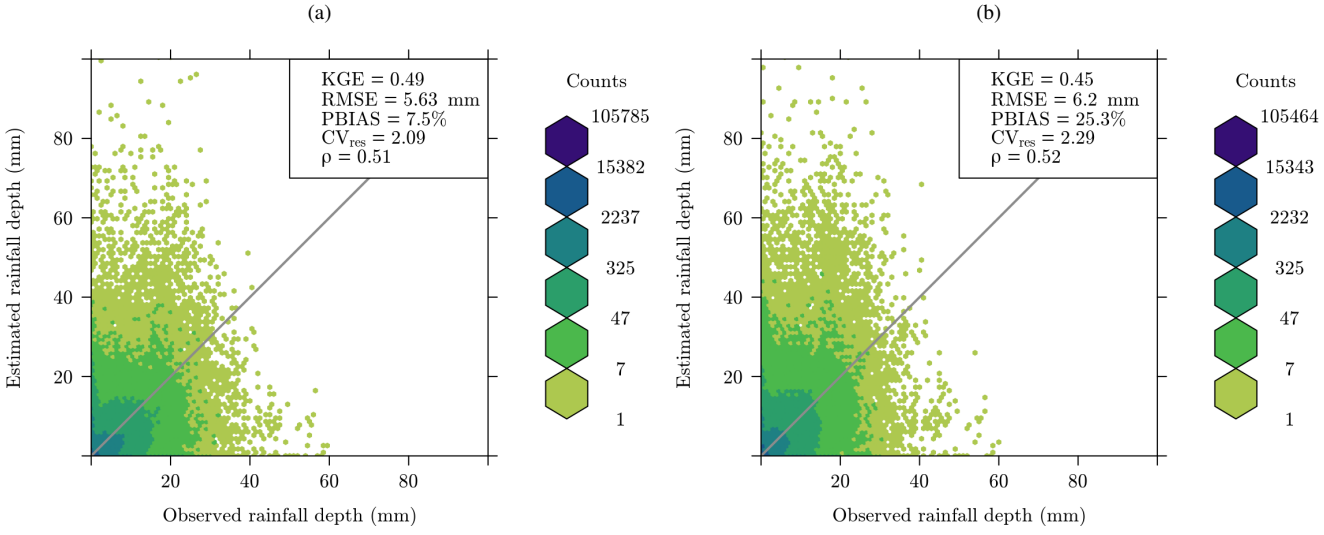

Figure 4. Daily path-averaged rainfall depth comparison of CML rainfall estimates against gauge-adjusted radar data: (a) rainfall retrieved using calibrated parameters; (b) rainfall retrieved using default parameters.

The main improvement is observed for the percent bias (PBIAS). Even if both parameter sets lead to overestimates compared to the reference, the rainfall depth retrieved when using the calibrated parameters shows 17.8 percentage points less overestimation compared to using the default parameters. In addition to ρ, the bias ratio (β) and the variability ratio (γ) are incorporated into the KGE metric (Equations (5)–(7)). For the default parameters β and γ are 1.25 and 1.11, respectively. For the calibrated parameters the values of β and γ are 1.07 and 1.12, respectively. All of the three KGE components have their ideal value at unity and the higher value of KGE when using the calibrated parameters is due to a better bias performance. Overall, the calibrated parameters outperform the default parameters.

Next, the performance of 15-minute path-averaged rainfall estimates is investigated. Table 5 summarizes RAINLINK's performance when the default and calibrated parameters are applied. For a complete evaluation we use different rainfall thresholds. The calibrated parameter set yields a better performance of RAINLINK in terms of RMSE, and CV_{res} for all thresholds. Except for the threshold "Reference > 1", KGE resulted in a better performance for the calibrated parameter set, as well. As for PBIAS, the default parameters outperform the calibrated ones for the thresholds "Reference > 0" and "Reference > 1", whereas the calibrated parameters show better performance for the remaining thresholds. One can also observe that, if a threshold is only applied to the reference, RAINLINK shows a large underestimation with respect to the reference. This underestimation is not observed if both RAINLINK and the reference are above the threshold. This indicates that the observed underestimation is due to RAINLINK estimating zero rain when the reference suggests that it is raining. This may be related to differences in spatial and temporal sampling, although we are not able to provide a conclusive explanation.

The only goodness-of-fit metric which results in a better performance of RAINLINK for the default parameters is ρ, although the improvement is slight. As a result of the optimization setup including the zero observations, these positive validation

https://doi.org/10.5194/amt-2021-34
Preprint. Discussion started: 12 March 2021

Atmospheric Measurement Techniques Discussions

Table 5. 15-minute path-averaged rainfall depth performance for different thresholds. Note: Reference is the gauge-adjusted radar data.

Thresholds of rainfall (mm)	RAINLINK with parameters	KGE	RMSE (mm)	PBIAS (%)	CV_{res}	ρ
Reference OR RAINLINK > 0	Default	0.24	1.04	31.80	2.57	0.31
	Calibrated	0.26	0.88	14.50	2.34	0.28
Reference OR RAINLINK > 0.1	Default	0.22	1.13	30.30	2.38	0.28
	Calibrated	0.23	0.98	12.20	2.13	0.24
Reference OR RAINLINK > 1	Default	−0.11	2.16	52.70	1.85	0.04
	Calibrated	−0.08	1.94	20.30	1.62	−0.05
Reference > 0	Default	−0.03	1.01	−34.30	1.30	0.49
	Calibrated	−0.02	0.92	−47.20	1.13	0.47
Reference > 1	Default	−0.36	1.92	−35.90	0.90	0.38
	Calibrated	−0.38	1.81	−51.00	0.76	0.36
No threshold (zero included)	Default	0.36	0.28	31.80	10.04	0.45
	Calibrated	0.41	0.24	14.50	8.86	0.43

315 outcomes are actually very similar and do not tend to really indicate improvements. With respect to data availability, the calibrated and default parameter sets contain 9.8% and 12.4% less observations than the entire data set, respectively.

Reevaluating the Overeem et al. (2016b) study employing default parameter values, de Vos et al. (2019) find 5.75%, 2.84, and 0.52 for PBIAS, CV_{res}, and ρ, respectively, for path-average 15-minute rainfall depths, and for link or radar larger than 0 mm. Differences with respect to the performance obtained here for the default parameter values (31.80%, 2.57, and 0.31 for 320 PBIAS, CV_{res}, and ρ, respectively) can be explained by the fact that the underlying data for both studies are from different periods, with different durations ($\sim$ 20 months for the months of February-October in de Vos et al. (2019) and 3 months for the months of June-August here).

Figure 5 shows density plots for all CML double-mass curves, i.e., the relation between the accumulations of rainfall retrieved by RAINLINK and that obtained from the gauge-adjusted radar reference. This figure shows that the class with the 325 highest occurrence coincides with the diagonal, indicating a reasonable agreement between the estimates and the observations. A considerable dispersion above the diagonal is found for both the calibrated and the default parameters. However, it is clear that with the calibrated parameters, this dispersion is less severe. This overestimation observed in the double-mass curves is in line with the PBIAS values reported earlier (Tab. 5). Identifying the extra attenuation as the main source of error, de Vos et al. (2019) report a similar behavior of the double-mass curves for instantaneous signal power sampling, although the considered 330 period and hence the meteorological circumstances are partly different.

So far small improvements in the rainfall retrievals are obtained when employing the calibrated parameters through the stochastic method Particle Swarm Optimization (PSO). However, analyzing the average over an area, in this case the Nether-

https://doi.org/10.5194/amt-2021-34
Preprint. Discussion started: 12 March 2021

Atmospheric Measurement Techniques Discussions

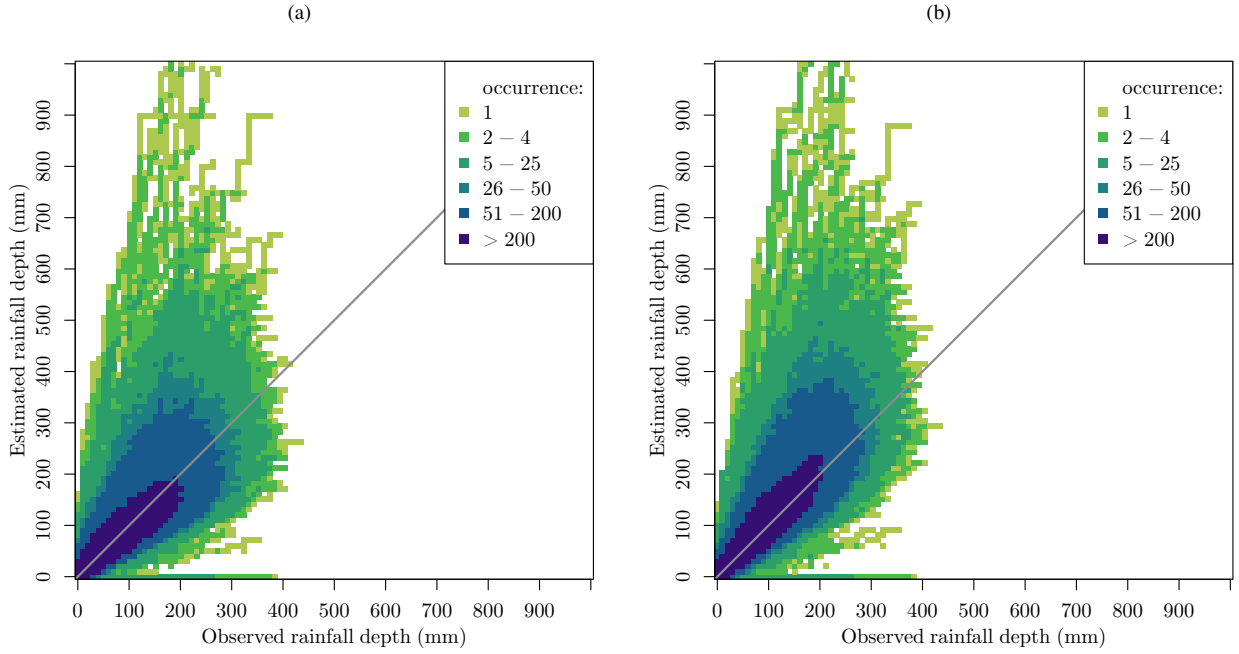

Figure 5. Density plots of the double mass curves of all individual CMLs with respect to the gauge-adjusted radar reference at 15-minute time intervals: (a) rainfall accumulations retrieved by RAINLINK with calibrated parameters; (b) rainfall accumulations retrieved by RAINLINK with default parameters.

lands, more substantial improvements are found. Figure 6 shows time series of the daily mean rainfall depth over the Netherlands, i.e., for each day the mean of all CML rainfall estimates is computed.

By employing the calibrated parameters, all metrics improved with respect to the default parameters. The values of KGE, RMSE, PBIAS, CV_{res}, and ρ improved from 0.60, 3.43 mm, 25.30%, 1.26, and 0.70 to 0.71, 2.89 mm, 7.50%, 1.07, and 0.72, respectively. Since the CML rainfall estimates are averaged over a $\sim$ 35,500 km^2 area, the PBIAS and β have the same values as reported before (Fig. 4). On the other hand, the variability and similarity (correlation), expressed by KGE components γ and ρ, respectively, are slightly better. For the areal time series obtained by employing calibrated parameters, γ and ρ are equal to 1 (1.01 for default) and 0.72 (0.70 for default), respectively. The value of γ being close to unity, confirms that the estimated rainfall time series vary to the same extent as the observed rainfall time series. Hence, as concluded from the path-averaged rainfall evaluation, the main improvement provided by the calibrated parameters as compared to the default parameters is a lower relative bias.

For both sets of parameters, calibrated and default, CML-derived rainfall estimates correspond reasonably well to the gauge-adjusted radar rainfall estimates. For path-averaged daily rainfall an improvement is found when calibrated parameter values are employed, especially in terms of relative bias. Results further improve when rainfall estimates are averaged over the entire

https://doi.org/10.5194/amt-2021-34
Preprint. Discussion started: 12 March 2021

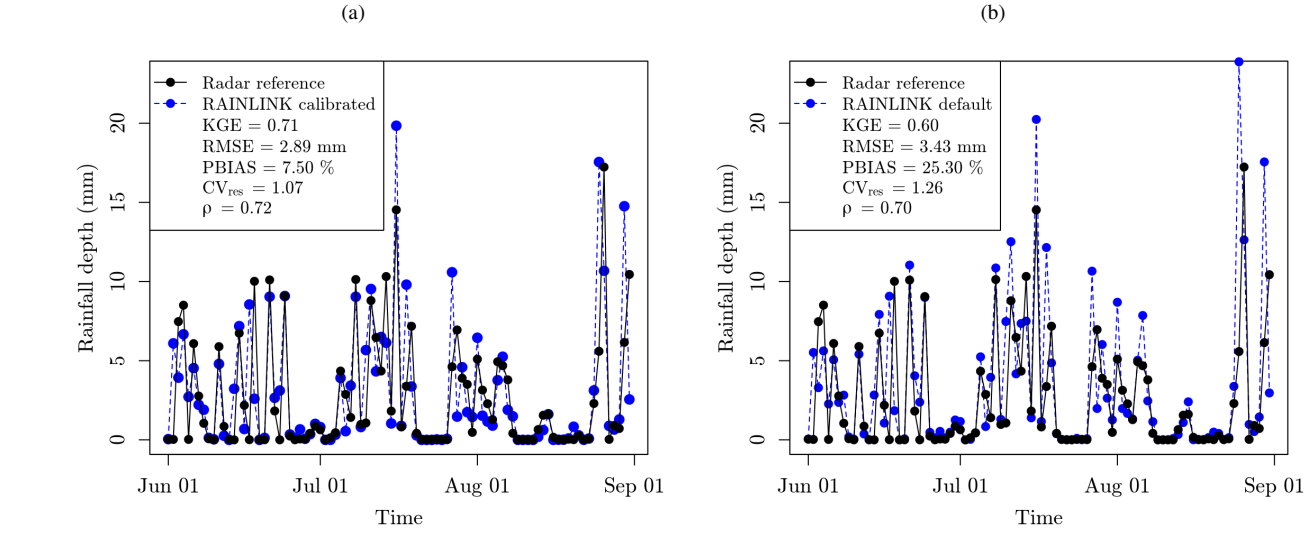

Figure 6. Comparison of the daily mean rainfall depth time series for the entire Netherlands during the summer months June, July and August 2012: (a) rainfall time series retrieved by RAINLINK with calibrated parameters; (b) rainfall time series retrieved by RAINLINK with default parameters.

Netherlands. Differences in calibrated parameter values with respect to the default ones may be caused by the calibration being performed over different events in June and July 2009 and in 2011 for the default parameters (Overeem et al., 2011, 2013).

3.3 Search space of parameters

For some parameters in Tables 1 and 2 a wider search space could have been chosen. For WD_{p2} and RR_{p2} a maximum value of 24 h was chosen, implying that data from the previous day are needed. Because the calibration dataset is not continuous, it was not feasible to use a larger value for WD_{p2}. In both cases 24 h seems reasonably long for a reliable computation. The maximum allowed value of 24 h for RR_{p2} may even be beneficial for the reference level determination. If this value would become longer than 24 h, varying meteorological conditions (e.g. related to changes in relative humidity) may affect the accuracy of the reference level determination, being less representative of the reference level just before a rainfall event. For the radius WD_{p3} the minimum value is 15 km. A lower value could be tested, but given the network density (Fig. 1), this is expected to lead to a (severe) reduction of available sub-links. This is because the wet-dry classification needs a minimum number of nearby links, which is more difficult to achieve in case of a smaller radius. The employed minimum value for WD_{p6} is already quite low. The wet-dry classification is expected to become more reliable when more sub-links are involved. Hence, it does not seem sensible to choose an even lower minimum value.

https://doi.org/10.5194/amt-2021-34
Preprint. Discussion started: 12 March 2021


Atmospheric Measurement Techniques Discussions

4 Conclusions

A novel and reliable method for the objective estimation of optimum parameter sets for RAINLINK and potentially for other CML-based rainfall retrieval algorithms has been presented and tested. Using a 12-day dataset, the calibration was performed by means of a stochastic approach, Particle Swarm Optimization (PSO), preceded by a sensitivity analysis selecting the parameters to be optimized. The optimized parameters were determined according to 95% confidence intervals for the "behavioral" solutions, i.e., those solutions performing better than the solution obtained by using the default parameters (Overeem et al., 2011, 2013, 2016a).

The validation of daily path-averaged CML rainfall estimates over three summer months reveals a reasonable improvement for the calibrated parameters compared to the default values. When daily path-averaged values are averaged over the entire surface area of the Netherlands, the improvement becomes much stronger. The aggregation over an area tends to limit the effects of representativeness errors in the rainfall estimates and yields information with an acceptable performance for hydrological and meteorological applications. This result is important, because in general hydrological and meteorological scales of application are defined over areas, i.e., climate zones, political and administrative regions, watersheds, and so forth. Compelling improvements were achieved not only in terms of the performance of CML rainfall estimates as such, but also with respect to the choice of parameter values, which are now underpinned in a more objective way.

In fact, we now have a way to analyze the sensitivity and optimize stochastically all parameters used in a rainfall retrieval algorithm. The proposed methodology is applicable for different CML networks, climates, and algorithms, where either rain gauge or (gauge-adjusted) radar data can be used as reference. In case of other sampling strategies than min/max the algorithm can be easily adapted. Ideally, optimized parameters would be obtained for different seasons. Hence, for each processing period a dedicated parameter set would be obtained.

Fencl et al. (2019) underline the importance of considering the rainfall properties in the quantification of wet antenna attenuation, where a fixed value may lead to overestimation of heavy rainfalls. This can lead to an increase in the computational cost however, especially in case of extensive CML datatsets. We also recommend to extend our algorithm by adding an extra goodness-of-fit criterion to the optimization regarding the sub-link data availability after running RAINLINK's processing steps (de Vos et al., 2019). This could lead to improved coverage of CML rainfall estimates. In general, quantifying the effect of processing steps on data availability is important.

As a recommendation, studies could be conducted by testing the convergence and performance of different goodness-of-fit measures in addition to the Kling-Gupta efficiency (Kling et al., 2012). Moreover, one could optimize the parameters using rain gauges near the CMLs as reference in order to exclude deviations that are sometimes found in radar rainfall observations. Moreover, representativeness errors between radars, measuring aloft, and CMLs, measuring near the Earth's surface, can affect comparisons between the two. This especially holds for short time intervals, as short as 15 minutes in this study.

In spite of having stochastic proprieties and aiming to explore the uncertainties affecting rainfall retrievals from CMLs, the approach proposed here is not a panacea. In regions without reliable rainfall ground-truth the calibration of rainfall retrieval algorithm parameters can be a challenge (Chwala and Kunstmann, 2019). Hence, we recommend the set-up of experiments

https://doi.org/10.5194/amt-2021-34
Preprint. Discussion started: 12 March 2021


Atmospheric Measurement Techniques Discussions

in regions with little ground-based rainfall information in order to optimize parameters for specific networks and climates, or even to improve rainfall retrieval algorithms such as RAINLINK themselves. As an alternative, parameters could be optimized in a well-gauged region having a similar climate and CML network as the ungauged region for which CML rainfall estimates are desired.

Comparing CML-derived rainfall maps and gauge-adjusted radar observations, Overeem et al. (2016b) found a better performance for the summer season than for the winter season in the Netherlands, among others due to the absence of snow and melting precipitation. The rainfall type during the Dutch summer is largely of a convective nature, bearing some resemblance with that in regions characterized by (sub)tropical climates, which often lack surface rainfall observations. As a consequence, we believe CML rainfall monitoring is especially promising for low- to middle-income countries, typically having (sub)tropical climates.

Acknowledgements. We gratefully acknowledge Ronald Kloeg and Ralph Koppelaar from T-Mobile NL for providing the cellular communication link data. This study was financially supported by the São Paulo Research Foundation (FAPESP) under the grant number 2017/09708-7.

Data availability. The CML data are available via https://doi.org/10.4121/uuid:323587ea-82b7-4cff-b123-c660424345e5. The gauge-adjusted radar data can be obtained at https://dataplatform.knmi.nl/catalog/datasets/index.html?x-dataset=rad_nl25_rac_mfbs_5min&x-dataset-version=2.0.

https://doi.org/10.5194/amt-2021-34
Preprint. Discussion started: 12 March 2021

Atmospheric Measurement Techniques Discussions

References

Abdelaziz, R. and Zambrano-Bigiarini, M.: Particle Swarm Optimization for inverse modeling of solute transport in fractured gneiss aquifer, Journal of Contaminant Hydrology, 164, 285–298, https://doi.org/10.1016/j.jconhyd.2014.06.003, 2014.

Atlas, D. and Ulbrich, C. W.: Path- and area-integrated rainfall measurement by microwave attenuation in the 1–3 cm band, Journal of Applied Meteorology, 16, 1322–1331, https://doi.org/10.1175/1520-0450(1977)016<1322:PAAIRM>2.0.CO;2, 1977.

Bianchi, B., van Leeuwen, P. J., Hogan, R. J., and Berne, A.: A variational approach to retrieve rain rate by combining information from rain gauges, radars, and microwave links, Journal of Hydrometeorology, 14, 1897–1909, https://doi.org/10.1175/JHM-D-12-094.1, 2013.

Bisselink, B., Zambrano-Bigiarini, M., Burek, P., and de Roo, A.: Assessing the role of uncertain precipitation estimates on the robustness of hydrological model parameters under highly variable climate conditions, Journal of Hydrology: Regional Studies, 8, 112–129, https://doi.org/10.1016/j.ejrh.2016.09.003, 2016.

Brauer, C. C., Overeem, A., Leijnse, H., and Uijlenhoet, R.: The effect of differences between rainfall measurement techniques on groundwater and discharge simulations in a lowland catchment, Hydrological Processes, 30, 3885–3900, https://doi.org/10.1002/hyp.10898, 2016.

Chwala, C. and Kunstmann, H.: Commercial microwave link networks for rainfall observation: Assessment of the current status and future challenges, Wiley Interdisciplinary Reviews: Water, 6, e1337, https://doi.org/10.1002/wat2.1337, 2019.

Chwala, C., Gmeiner, A., Qiu, W., Hipp, S., Nienaber, D., Siart, U., Eibert, T., Pohl, M., Seltmann, J., Fritz, J., and Kunstmann, H.: Precipitation observation using microwave backhaul links in the alpine and pre-alpine region of Southern Germany, Hydrology and Earth System Sciences, 16, 2647–2661, https://doi.org/10.5194/hess-16-2647-2012, 2012.

Clerc, M.: Standard Particle Swarm Optimisation, https://hal.archives-ouvertes.fr/hal-00764996, 15 pages, 2012.

de Vos, L., Overeem, A., Leijnse, H., and Uijlenhoet, R.: Rainfall estimation accuracy of a nation-wide instantaneously sampling commercial microwave link network: error-dependency on known characteristics, Journal of Atmospheric and Oceanic Technology, https://doi.org/10.1175/JTECH-D-18-0197.1, 2019.

Fencl, M., Rieckermann, J., Sýkora, P., Stránský, D., and Bareš, V.: Commercial microwave links instead of rain gauges: fiction or reality?, Water Science & Technology, 71, 31, https://doi.org/10.2166/wst.2014.466, 2015.

Fencl, M., Valtr, P., Kvicera, M., and Bares, V.: Quantifying wet antenna attenuation in 38-GHz commercial microwave links of cellular backhaul, IEEE Geoscience and Remote Sensing Letters, 16, 514–518, https://doi.org/10.1109/LGRS.2018.2876696, 2019.

Graf, M., Chwala, C., Polz, J., and Kunstmann, H.: Rainfall estimation from a German-wide commercial microwave link network: optimized processing and validation for 1 year of data, Hydrol. Earth Syst. Sci., 24, 2931–2950, https://doi.org/10.5194/hess-24-2931-2020, 2020.

GSMA: Mobile technology for rural climate resilience: The role of mobile operators in bridging the data gap, https://www.gsma.com/mobilefordevelopment/wp-content/uploads/2019/10/GSMA_AgriTech_Climate_Report.pdf, tech. Rep., London, UK, retrieved 13 August 2020, 2019.

Kling, H., Fuchs, M., and Paulin, M.: Runoff conditions in the upper Danube basin under an ensemble of climate change scenarios, Journal of Hydrology, 424-425, 264–277, https://doi.org/10.1016/j.jhydrol.2012.01.011, 2012.

Leijnse, H., Uijlenhoet, R., and Stricker, J. N. M.: Rainfall measurement using radio links from cellular communication networks, Water Resources Research, 43, https://doi.org/10.1029/2006WR005631, 2007.

Leijnse, H., Uijlenhoet, R., and Stricker, J.: Microwave link rainfall estimation: effects of link length and frequency, temporal sampling, power resolution, and wet antenna attenuation, Advances in Water Resources, 31, 1481–1493, https://doi.org/10.1016/j.advwatres.2008.03.004, 2008.

https://doi.org/10.5194/amt-2021-34
Preprint. Discussion started: 12 March 2021

Atmospheric Measurement Techniques Discussions

Liberman, Y., Samuels, R., Alpert, P., and Messer, H.: New algorithm for integration between wireless microwave sensor network and radar for improved rainfall measurement and mapping, Atmospheric Measurement Techniques, 7, 3549–3563, https://doi.org/10.5194/amt-7-3549-2014, 2014.

Matott, L. S., Babendreier, J. E., and Purucker, S. T.: Evaluating uncertainty in integrated environmental models: a review of concepts and tools, Water Resources Research, 45, 1–14, https://doi.org/10.1029/2008WR007301, 2009.

Messer, H.: Environmental monitoring by wireless communication networks, Science, 312, 713–713, https://doi.org/10.1126/science.1120034, 2006.

Messer, H. and Sendik, O.: A new approach to precipitation monitoring: a critical survey of existing technologies and challenges, IEEE Signal Processing Magazine, 32, 110–122, https://doi.org/10.1109/MSP.2014.2309705, 2015.

Olsen, R., Rogers, D., and Hodge, D.: The aR^b relation in the calculation of rain attenuation, IEEE Transactions on Antennas and Propagation, 26, 318–329, https://doi.org/10.1109/TAP.1978.1141845, 1978.

Overeem, A., Buishand, T. A., and Holleman, I.: Extreme rainfall analysis and estimation of depth-duration-frequency curves using weather radar, Water Resources Research, 45, 1–15, https://doi.org/10.1029/2009WR007869, 2009a.

Overeem, A., Holleman, I., and Buishand, A.: Derivation of a 10-year radar-based climatology of rainfall, Journal of Applied Meteorology and Climatology, 48, 1448–1463, https://doi.org/10.1175/2009JAMC1954.1, 2009b.

Overeem, A., Leijnse, H., and Uijlenhoet, R.: Measuring urban rainfall using microwave links from commercial cellular communication networks, Water Resources Research, 47, https://doi.org/10.1029/2010WR010350, 2011.

Overeem, A., Leijnse, H., and Uijlenhoet, R.: Country-wide rainfall maps from cellular communication networks, Proceedings of the National Academy of Sciences, 110, 2741–2745, https://doi.org/10.1073/pnas.1217961110, 2013.

Overeem, A., Leijnse, H., and Uijlenhoet, R.: Retrieval algorithm for rainfall mapping from microwave links in a cellular communication network, Atmospheric Measurement Techniques, 9, 2425–2444, https://doi.org/10.5194/amt-9-2425-2016, 2016a.

Overeem, A., Leijnse, H., and Uijlenhoet, R.: Two and a half years of country-wide rainfall maps using radio links from commercial cellular telecommunication networks, Water Resources Research, 52, 8039–8065, https://doi.org/10.1002/2016WR019412, 2016b.

Overeem, A., Leijnse, H., and de Vos Lotte: RAINNLINK: Retrieval algorithm for rainfall mapping from microwave links in a cellular communication network, https://github.com/overeem11/RAINLINK, R package version 1.14, 2019.

Peel, M. C., Finlayson, B. L., and McMahon, T. A.: Updated world map of the Köppen-Geiger climate classification, Hydrology and Earth System Sciences, 11, 1633–1644, https://doi.org/10.5194/hess-11-1633-2007, 2007.

Pijl, A., Brauer, C. C., Sofia, G., Teuling, A. J., and Tarolli, P.: Hydrologic impacts of changing land use and climate in the Veneto lowlands of Italy, Anthropocene, 22, 20–30, https://doi.org/10.1016/j.ancene.2018.04.001, 2018.

R Core Team: R: A Language and Environment for Statistical Computing, Version 3.4.4, http://www.R-project.org/, 2018.

Rios Gaona, M. F., Overeem, A., Raupach, T. H., Leijnse, H., and Uijlenhoet, R.: Rainfall retrieval with commercial microwave links in São Paulo, Brazil, Atmospheric Measurement Techniques, 11, 4465–4476, https://doi.org/10.5194/amt-11-4465-2018, 2018.

Roversi, G., Alberoni, P. P., Fornasiero, A., and Porcù, F.: Commercial microwave links as a tool for operational rainfall monitoring in Northern Italy, Atmos. Meas. Tech., 13, 5779—-5797, https://doi.org/10.5194/amt-13-5779-2020, 2020.

Schneider, U., Finger, P., Meyer-Christoffer, A., Ziese, M., and Becker, A.: Global Precipitation Analysis Products of the GPCC, Tech. Rep. 8, National Meteorological Service of Germany, Offenbach am Main, ftp://ftp-anon.dwd.de/pub/data/gpcc/PDF/GPCC_intro_products_lastversion.pdf, 2018.

https://doi.org/10.5194/amt-2021-34
Preprint. Discussion started: 12 March 2021

Smiatek, G., Keis, F., Chwala, C., Fersch, B., and Kunstmann, H.: Potential of commercial microwave link network derived rainfall for river runoff simulations, Environmental Research Letters, 12, 034 026, https://doi.org/10.1088/1748-9326/aa5f46, 2017.

Sohail Afzal, M., Shah, S. H. H., Cheema, M. J. M., and Ahmad, R.: Real time rainfall estimation using microwave signals of cellular communication networks: a case study of Faisalabad, Pakistan, Hydrology and Earth System Sciences Discussions, pp. 1–20, https://doi.org/10.5194/hess-2017-740, 2018.

Sokal, R. R. and Michener, C. D.: A statistical method for evaluating systematic relationships, University of Kansas Scientific Bulletin, 28, 1409–1438, https://ci.nii.ac.jp/naid/10011579647/en/, 1958.

Sun, Q., Miao, C., Duan, Q., Ashouri, H., Sorooshian, S., and Hsu, K.-L.: A review of global precipitation data sets: data sources, estimation, and intercomparisons, Reviews of Geophysics, 56, 79–107, https://doi.org/10.1002/2017RG000574, 2018.

Uijlenhoet, R., Overeem, A., and Leijnse, H.: Opportunistic remote sensing of rainfall using microwave links from cellular communication networks, WIREs Water, 5, 1–15, https://doi.org/10.1002/wat2.1289, 2018.

Upton, G., Holt, A., Cummings, R., Rahimi, A., and Goddard, J.: Microwave links: The future for urban rainfall measurement?, Atmospheric Research, 77, 300–312, https://doi.org/10.1016/j.atmosres.2004.10.009, 2005.

Van Griensven, A., Meixner, T., Grunwald, S., Bishop, T., Diluzio, M., and Srinivasan, R.: A global sensitivity analysis tool for the parameters of multi-variable catchment models, Journal of Hydrology, 324, 10–23, https://doi.org/10.1016/j.jhydrol.2005.09.008, 2006.

Wilcoxon, F.: Individual comparisons by ranking methods, Biometrics Bulletin, 1, 80, https://doi.org/10.2307/3001968, 1945.

Zinevich, A., Messer, H., and Alpert, P.: Frontal rainfall observation by a commercial microwave communication network, Journal of Applied Meteorology and Climatology, 48, 1317–1334, https://doi.org/10.1175/2008JAMC2014.1, 2009.